REGULAR ARTICLE

blood advances

Structural analysis of platelet fragments and extracellular vesicles produced by apheresis platelets during storage

Silvia H. De Paoli,[1,*] Mehulkumar Patel,[1,2,*] Oumsalama K. Elhelu,[1] Ivan D. Tarandovskiy,[1,3] Tseday Z. Tegegn,[1] and Jan Simak[1]

[1]Laboratory of Cellular Hematology, Office of Blood Research and Review, Center for Biologics Evaluation and Research, [2]Office of Science and Engineering Laboratories, Center for Devices and Radiological Health, and [3]Hemostasis Branch, Office of Therapeutic Products, Center of Biologics Evaluations and Research, US Food and Drug Administration, Silver Spring, MD

Key Points

- We characterized and classified the membranous particle content of apheresis PLTs for transfusion during their storage.
- After 7 days storage, the amount of degranulated PLTs, PLT membrane ghosts, and vesicles produced by apheresis PLTs increases.

Platelets (PLTs) for transfusion can be stored for up to 7 days at room temperature (RT). The quality of apheresis PLTs decreases over storage time, which affects PLT hemostatic functions. Here, we characterized the membranous particles produced by PLT storage lesion (PSLPs), including degranulated PLTs, PLT ghosts, membrane fragments, and extracellular membrane vesicles (PEVs). The PSLPs generated in apheresis platelet units were analyzed on days 1, 3, 5, and 7 of RT storage. A differential centrifugation and a sucrose density gradient were used to separate PSLP populations. PSLPs were characterized using scanning and transmission electron microscopy (EM), flow cytometry (FC), and nanoparticle tracking analysis (NTA). PSLPs have different morphologies and a broad size distribution; FC and NTA showed that the concentration of small and large PSLPs increases with storage time. The density gradient separated 3 PSLP populations: (1) degranulated PLTs, PLT ghosts, and large PLT fragments; (2) PEVs originated from PLT activation and organelles released by necrotic PLTs; and (3) PEV ghosts. Most PSLPs expressed phosphatidyl serine and induced thrombin generation in the plasma. PSLPs contained extracellular mitochondria and some had the autophagosome marker LC3. PSLPs encompass degranulated PLTs, PLT ghosts, large PLT fragments, large and dense PEVs, and low-density PEV ghosts. The activation-related PSLPs are released, particularly during early stage of storage (days 1-3), and the release of apoptosis- and necrosis-related PSLPs prevails after that. No elevation of LC3- and TOM20-positive PSLPs indicates that the increase of extracellular mitochondria during later-stage storage is not associated with PLT mitophagy.

Introduction

Apheresis platelets (PLTs) can be stored for 7 days at ambient temperatures, in a range from 20 to 24°C, under constant gentle agitation,[1] conditions that lead to PLT storage lesion (PSL).

PSL is a term first introduced by Murphy and Gardner[2] to describe deleterious changes observed in PLTs during storage, such as an increase in lactate levels, decrease in pH, loss of surface membrane glycoproteins, particularly glycoprotein Ib, and reduced aggregation responses to adenosine diphosphate and collagen. Storage lesion limits the apheresis PLT shelf-life and is associated with decreased in vivo PLT recovery, survival, and hemostatic activity after transfusion.[3,4]

Submitted 1 August 2023; accepted 4 November 2023; prepublished online on *Blood Advances* First Edition 15 November 2023. https://doi.org/10.1182/bloodadvances.2023011325.

*S.H.D.P. and M.P. contributed equally to this article.

Data are available on request from the corresponding author, Jan Simak (jan.simak@fda.hhs.gov).

The full-text version of this article contains a data supplement.

The mechanisms responsible for PSL are multifactorial and include the physical stress from PLT collection, processing, storage, and manipulation after collection.[5,6] Aside from the physical stresses, biochemical changes due to apheresis PLT aging contribute to PSL.[7]

Although anucleate, PLTs have the capacity to undergo programmed cell death.[7-11] During storage, PLTs present several features of apoptosis,[12-14] such as cytoskeletal disruption, vesiculation, caspase activation, and phosphatidylserine (PS) exposure.[12]

Biochemical processes associated with PSL have also been linked to PLT necrosis,[15] particularly those responsible for severe mitochondrial damage, swelling of plasma and organelle membranes, changes in intracellular pH, membrane lysis and release of lactate dehydrogenase, and loss of sialylated glycans.[16-19] In fact, the possibility of stored platelets undergoing secondary necrosis may partly explain the inability of apoptosis inhibitors to maintain the viability of stored PLT products.[7]

Autophagy is another operational programmed cell death pathway in PLTs.[20] Autophagy is induced upon PLT activation and is essential for hemostasis and thrombosis,[21] and mitophagy in PLTs has been demonstrated in hypoxic conditions,[22] diabetes,[23] and starvation.[24] However, the contribution of autophagy/mitophagy to the PSL remains to be established.

The biological effects of the releasates in the apheresis PLT supernatant are a current topic of research.[25] For instance, Cognasse et al demonstrated that the supernatants of stored PLTs contain potential immunomodulatory factors,[26] and Sut et al showed that platelet concentrate supernatants alter endothelial cell messenger RNA, causing cell activation.[27] In those studies, attention was given to the soluble molecules present in the apheresis PLT supernatants, such as cytokines, chemokines, and so on. In this study, we investigated membranous particles that are products of PSL (PSLPs), including degranulated PLTs (DPLTs), PLT ghosts (empty platelet plasma membranes, free of granules, other organelles, and cytoplasmic content), membrane fragments, and PLT extracellular membrane vesicles (PEVs). The fate of particles in circulation, including cellular uptake, depends on the particle size and surface properties.[28-33] Thus, the physicochemical features of circulating PSLPs are expected to influence their interactions with cells of the vascular system and, consequently, their ability to transfer bioactive cargo molecules.[34,35]

Materials and methods

Texas Red 1,2-dihexadecanoyl-sn-glycero-3-phosphoethanolamine (DHPE) was from Thermo Fisher Scientific. Fluorescein isothiocyanate (FITC)-conjugated LC3 antibody kit (no. FCCH100171, clone 4E12), bovine serum albumin, prostaglandin E1, 1,6-diphenyl-1,3,5-hexatriene (DPH), and sucrose were from Sigma. Anti-human Tom20 (F-10) Alexa Fluor 647-conjugated (no. sc-17764 AF647) was from Santa Cruz Biotechnology. FITC mouse anti-human CD41a (clone HIP8), phycoerythrin (PE) mouse anti-human CD41a (clone HIP8), PE mouse anti-human CD62P (clone AK-4), PE-conjugated mouse immunoglobulin G1 (IgG1; clone MOPC-21; isotype control), and FITC-conjugated mouse IgG1 (clone MOPC-21; isotype control) were from BD Pharmingen. Lactadherin-FITC Labeled (BLAC-FITC) was from Haematologic Technologies. Osmium tetroxide, paraformaldehyde, glutaraldehyde, and Embed 812 were from Electron Microscopy Sciences.

Collection and storage of apheresis PLTs

Apheresis PLTs from 12 healthy donors (1 110 000 ± 168 000 platelets per μL) were collected using an Amicus cell separator (Fresenius Kabi) and provided by the Department of Transfusion Medicine, National Institutes of Health (Bethesda, MD). The platelet units were procured by the Center for Biologics Evaluation and Research institutional review board, which allows only the release of deidentified material. All units were collected and stored in plasma at room temperature (RT; 20 to 24°C) on a PF48h Horizon Series Platelet Agitator (Helmer Scientific; flatbed platelet agitator, agitation speed 60 cycles/min, stroke length 3.8 cm) for 7 days with continual side-to-side motion.

Isolation of PSLPs

From apheresis PLT units, 5 mL samples were collected on days 1, 3, 5, and 7 of storage; prostaglandin E1 with a final 1μM concentration was added to the PLT samples before centrifugation at 1000 *g* for 30 minutes at RT to isolate intact PLTs from the supernatant containing PSLPs.

Flow cytometry

The supernatant containing PSLPs was diluted with 1.5% bovine serum albumin/phosphate-buffered saline (PBS) to get 1000 to 2000 events per second during analysis. Then, 300 μL of diluted supernatant was incubated for 20 minutes at RT with a saturating concentration of monoclonal antibodies against CD41a (FITC/PE, 10 μL; 1:10), CD62P (PE, 10 μL; 1:10), TOM20 (Alexa 647, 10 μL; 1:5), LC3 (FITC, 5 μL), or lactadherin (FITC, 10 μL; 1:5), or with the membrane labeling DHPE (Texas Red, 20 μL; 1:10). PSLPs were sedimented at 30 000 *g* for 30 minutes at 4°C and washed with 1 mL of PBS. The pellet was resuspended in 300 μL of PBS and immediately analyzed using an LSRII flow cytometer (BD Biosciences). Respective IgG isotype antibody controls and nonlabeled samples were used as controls. To estimate the size of PSLPs, the flow cytometer was calibrated using the ApogeeMix calibration beads (Apogee Flow Systems). TruCount TM beads (Becton Dickinson) were used to evaluate the flow rate and PSLP counts. Data analysis was performed using FlowJo software. All the antibodies were titrated to ensure a saturating concentration, and we analyzed at least 10 000 gated PSLPs for each sample.

Sucrose density gradient

PSLPs pelleted from 100 mL of apheresis PLT units were subjected to a sucrose density gradient. Sucrose gradients were prepared in 10 mL Beckman centrifuge tubes in 1 mL layers of sucrose solution in tris(hydroxymethyl)aminomethane buffer (0.21, 0.46, 0.56, 0.73, 0.88, 1.02, 1.10, 1.22, 1.33, 1.46, 1.54, and 2.25 mol/L) to create a density (*d*) gradient of 1.0259 to 1.2575 g/mL. After ultracentrifugation (Beckman Counter) at 100 000 *g* for 14 hours, the 3 populations of PSLPs were collected and analyzed by flow cytometry (FC) by diluting 50 μL of each fraction in 1 mL of Tyrode buffer before incubation with antibodies. Fractions were also prepared for transmission electron microscopy (TEM).

Field emission scanning electron microscopy

Samples were fixed with 4% paraformaldehyde and 2% glutaraldehyde, followed by dehydration and drying at RT. Samples were

sputter-coated with a thin film of gold. The change in morphology of platelets at different days of storage was evaluated by analyzing scanning electron microscopy (SEM) images using ImageJ software and calculating the circularity value (values 1.0-0.0 indicate a perfect circle to an increasingly elongated polygon shape).[36]

TEM

Samples were fixed with 2.5% paraformaldehyde and 2.5% glutaraldehyde, followed by 1% osmium staining; samples were dehydrated and resin-embedded before ultramicrotomy.

Fluorescence polarization

Apheresis PLTs were incubated with 1 μM DPH for 30 minutes. A total of 30 nmol/L of membrane fluidizer halothane was used as a positive control. The fluorescence of DPH was read at 360 or 420 nm.

TG test

Thrombin generation (TG) test was performed as described previously,[37] using 0.2 pM tissue factor, pooled healthy plasma, $CaCl_2$, and a fluorogenic Z-Gly-Gly-Arg-7-amino-4-methylcoumarin substrate.

Statistical analysis

FC data are expressed as the fold change in the count of small and large PSLPs normalized to that of day 1 of storage (mean ± standard error) ($^{\#}P < .01$; $^{*}P < .05$; N = 12). FC data for the 3 PSLP populations isolated by sucrose gradient are presented as mean + standard deviation. The results were calculated from at least 3 independent experiments; FP data are presented as mean + standard deviation. One-way analysis of variance was used; P values < 0.05 were considered significant.

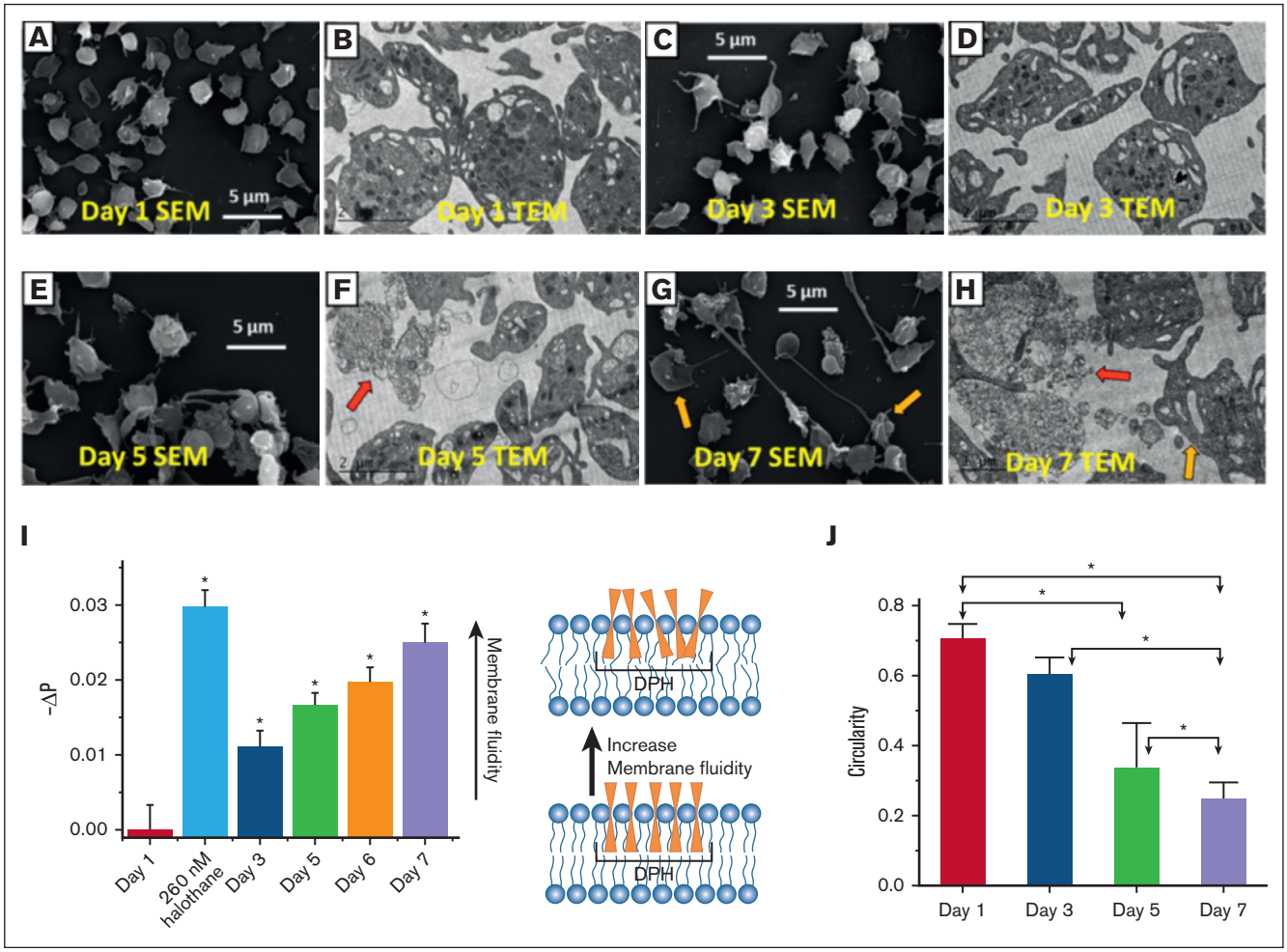

Figure 1. Morphologic and ultrastructural analysis of apheresis PLTs during storage. Representative SEM and TEM images of apheresis PLTs on day 1 (A-B), day 3 (C-D), day 5 (E-F), and day 7 (G-H) of storage. A reduction in DPH fluorescence polarization (FP) indicates an enhancement of PLT membrane fluidity (I). A decrease in the circularity value (mean ± standard error [SE], n ≥ 70 PLTs) of apheresis PLTs from days 1 to 7 indicates that PLTs are undergoing a shape change from circular to increasingly elongated shape. Platelet units from 3 different donors were used in the electron microscopy study. PLTs undergo shape changes, degranulation, and gradual loss of internal structures and membrane integrity, especially on days 5 and 7 of storage. Red arrows indicate necrotic PLTs (fragmented membrane release of intracellular organelles). Orange arrows indicate apoptotic PLTs (intact membrane, blebbing, filopodia extrusion, and release of PEVs).

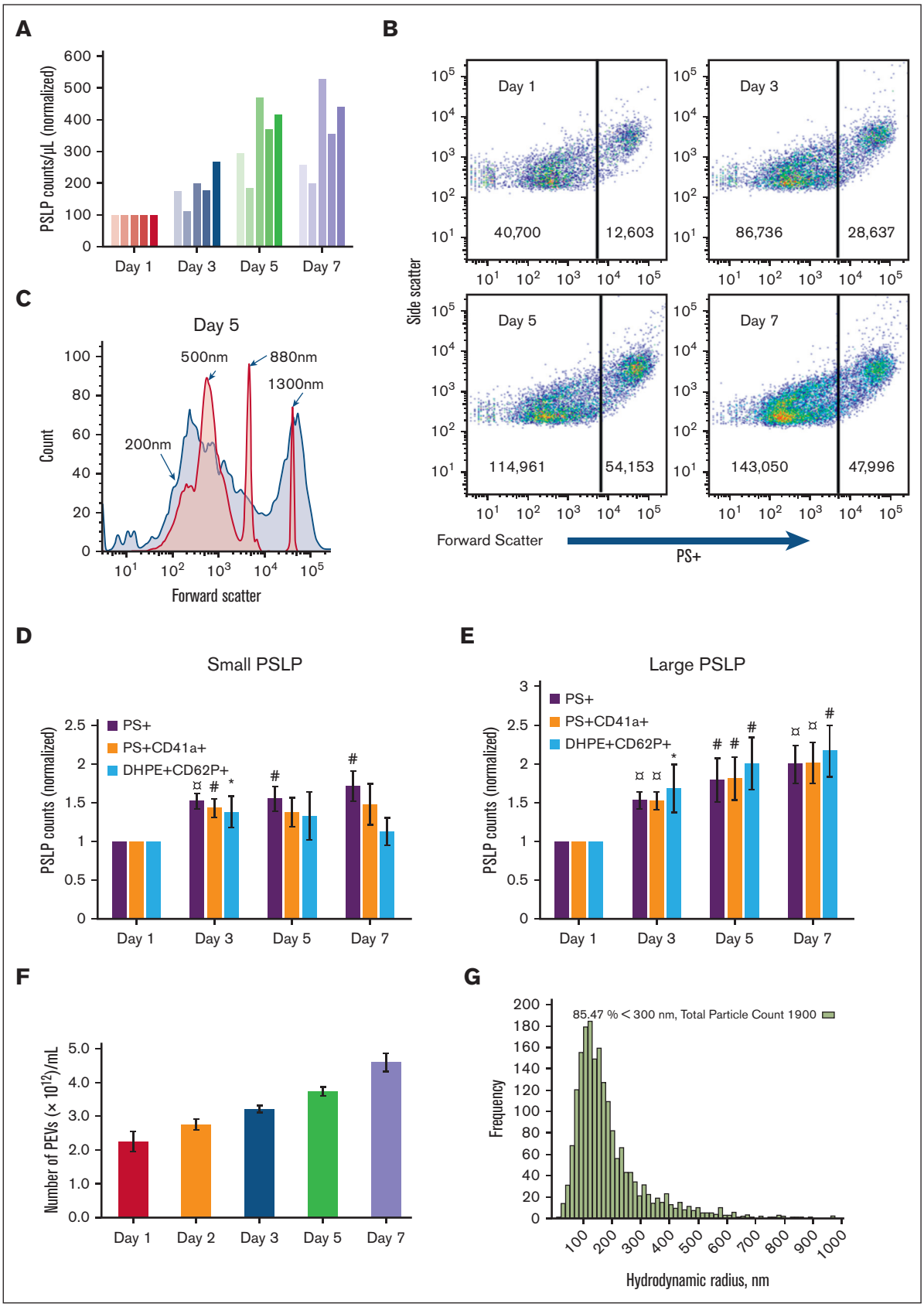
A
PSLP counts/µL (normalized)
600
500
400
300
200
100
0
Day 1
Day 3
Day 5
Day 7
B
Day 1
40,700
12,603
Day 3
86,736
28,637
Day 5
114,961
54,153
Day 7
143,050
47,996
Side scatter
Forward Scatter
PS+
C
Day 5
500nm
880nm
1300nm
200nm
Count
Forward scatter
D
Small PSLP
PS+
PS+CD41a+
DHPE+CD62P+
PSLP counts (normalized)
E
Large PSLP
PS+
PS+CD41a+
DHPE+CD62P+
PSLP counts (normalized)
F
Number of PEVs (× 10^12)/mL
Day 1
Day 2
Day 3
Day 5
Day 7
G
85.47 % < 300 nm, Total Particle Count 1900
Frequency
Hydrodynamic radius, nm

Figure 2.

Results

Characterization of apheresis PLTs after 1 to 7 days of storage

To characterize the PSLPs present in apheresis PLT products, apheresis PLT units were collected and stored at RT under gentle agitation for up to 7 days, according to standard guidelines.[38,39] Centrifugation of apheresis PLTs at 1000 *g* for 30 minutes allowed separation of intact PLTs for the characterization of the supernatant containing the PSLPs.

The effect of RT storage on apheresis PLT morphology was analyzed by electron microscopy. SEM topographic images (Figure 1A,C,E,G) and calculated circularity values (Figure 1J) of apheresis PLTs at different days reveal that aging apheresis PLTs undergo shape changes that include pseudopodia formation, membrane fragmentation, and PEV release; those observations were confirmed by TEM ultrastructural images (Figure 1B,D,F,H). TEM shows the presence of apoptotic (blebbing and filopodia extrusion) and necrotic (fragmented membrane release of intracellular organelles) PLTs, especially on days 5 and 7 of storage.

The physical state of apheresis PLT membranes during storage was evaluated by fluorescence polarization (FP) of the DPH probe,[40] shown in Figure 1I. RT storage causes disruption of membrane lipid packing, as indicated by the observed increase in membrane fluidity (or decrease in viscosity).

PSLP amount increases while PLTs are being stored

The number of PSLPs in the apheresis PLT supernatant increases with storage time, as measured by Coulter counting (Figure 2A) and FC (Figure 2B). Although the Coulter counter detects only large PSLPs, FC demonstrates that PSLPs have a broad size distribution that ranges from 200 nm to 5 µm. Figure 2C shows a representative forward scatter (FSC) histogram plot of PSLPs from PLT supernatant on day 5 of storage overlapped with the FSC histogram plots of silica standard size particles. As shown in Figure 2B, 2 major PSLP populations were identified and gated at the FSC peak of the 880 nm silica particles for further FC data analysis. Figure 2D-E show a steady increase in PS^+ and PS^+CD41^+ PSLPs in both small PSLP (200-880 nm) and large PSLP (880 nm-5 µm) populations with storage time. The number of large PS^+CD62P^+ PSLPs also increases with storage time. However, the number of small PS^+CD62P^+ PSLPs increases from day 1 to day 3 of storage only. Nanoparticle tracking analysis confirmed the elevation of PSLP concentration during storage (Figure 2F-G).

The morphologies and broad size distribution of the PSLPs are demonstrated by SEM images of apheresis PLT supernatants from days 1, 3, 5, and 7 of storage, presented in Figure 3A, B, C,D, respectively.

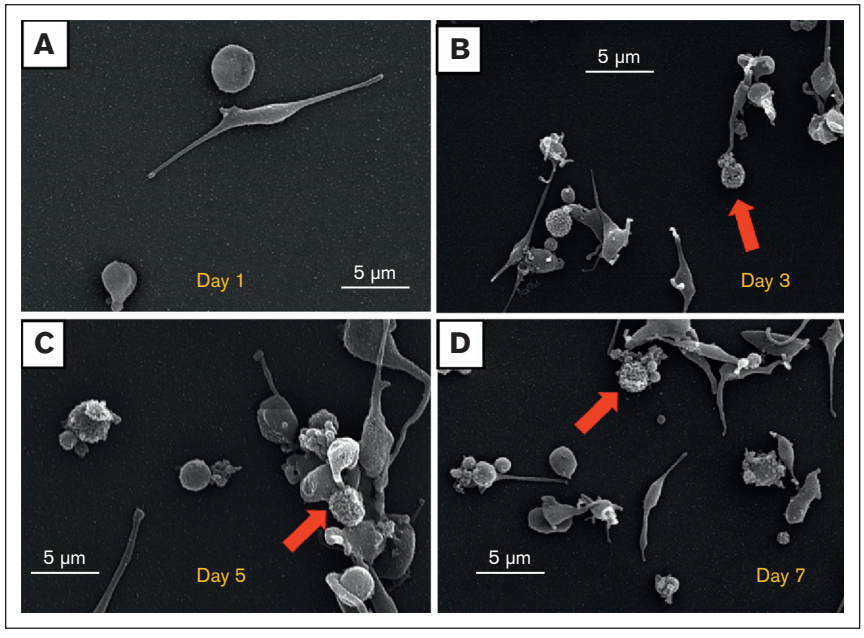

Figure 3. Apheresis PLT supernatant is composed of PSLPs with a broad size distribution. SEM images of PSLPs present in apheresis PLT supernatant on days 1 (A), 3 (B), 5 (C), and 7 (D). PLTs with fragmented membranes are indicated by red arrow.

Figure 2. The count of PSLPs increases during storage of apheresis PLTs at RT. (A) PSLP counts measured by Coulter counter for 5 individual apheresis PLT products. (B) FC scatter plots of PSLPs at days 1, 3, 5, and 7 of storage. (C) Representative FC size distribution plot of PSLPs on day 5 storage (red histogram represents silica standard size particles). FC-based counts of small (D) and large (E) PSLPs up to day 7 of storage (N = 12). FC data are expressed as the fold change in the count of small and large PEVs normalized to that of the day 1 platelet bag (mean ± SE) (¤$P < .001$; #$P < .01$; *$P < .05$; N = 12). (F) Nanoparticle tracking analysis (NTA) of PSLPs (N = 5). (G) Representative NTA histogram shows the broad size distribution of PSLPs.

PSLPs are highly diverse by their density and morphology

For further characterization, PSLPs isolated from apheresis PLT supernatant on day 7 of storage were pelleted by centrifugation at 30 000 *g* for 20 minutes and subjected to a sucrose density gradient at 100 000 *g* at 4°C for 14 hours. As shown in Figure 4A, 3 major populations of PSLPs were isolated and imaged by TEM. Figure 4B is a representative image of the denser PSLP population collected at $d = 1.14\text{-}1.17$ g/mL band, which is composed of partially DPLTs and large electron-dense PEVs; the membranes of the some DPLTs are fragmented, and release of intracellular organelles is observed. Figure 4C is a representative image of the population collected at $d = 1.09\text{-}1.13$ g/mL band composed of large and electron-dense PEVs with and without intact membranes. Figure 4D represents the population collected at the top layer of the sucrose gradient, composed of electron-translucent vesicles with a very low-density ($d = 1.02\text{-}1.06$ g/mL band).

The PSLP populations isolated by the density gradient were labeled for PS, CD41a, and CD62P and analyzed by FC. Figure 5A shows that on day 7 of storage, most of the ghost PSLPs are <700 nm (Figure 5A) and that the denser PSLPs are composed of 2 population with size ranges of 200 to 700 nm and 700 nm to 5 µm, as compared with silica standard size particles. Figure 5D shows that the number of PS^+CD41a^+ PSLPs and PS^+CD62P^+ PSLPs increases with the population density.

To verify the presence of PS on the PSLP surface, which is relevant for procoagulant activity, TG assay was performed. All PSLP populations isolated by the sucrose gradient are procoagulant. The TG activity was inhibited by blocking PS by adding 10 µM lactadherin (Figure 5E-F). We demonstrated strong inhibition of TG by lactadherin; however, in the case of dense PEVs, a little residual PS was still present in the system, likely indicating that the lactadherin concentration was not high enough to block all PS on the large membrane surface area of the dense PEV preparation. supplemental Figure 1 shows that at least 97% of PSLPs label for PS. PSLPs with disrupted membranes allow for lactadherin binding to PS in the inner membrane leaflet.

Apheresis PLTs release mitochondria during storage

The release of mitochondria (MITO) by apheresis PLTs during storage was indicated by TEM. Figure 6A, a representative TEM image of apheresis PLTs stored for 7 days, shows extracellularly enlarged MITO with irregular cristae structures. FC analysis of PSLPs labeled with the mitochondrial marker TOM20 shows that the number of PS^+TOM20^+ PSLP count increases with storage time, as shown in Figure 6C. The TEM image presented in Figure 6B clearly shows ongoing mitophagy on apheresis PLTs on day 3 of storage. To evaluate the role of autophagy/mitophagy on the release of MITO during storage, PSLPs were labeled with the autophagosome marker LC3. Figure 6C indicates the presence of mitophagy associated PSLPs ($TOM20^+LC3^+$ PSLPs and $DHPE^+LC3^+TOM20^+$ PSLPs), which do not significantly increase with storage time.

Discussion

Based on our observations and previously published work,[41] we propose that the PSLP generation evolves from PLT activation, apoptosis, necrosis, and autophagy, as described in Figure 7. Although the release of PLT extracellular vesicles (membrane microparticles) during PLT storage for transfusion has been previously investigated, very few data exist about a structural analysis of all membranous products of PSL. This study is focused not only on PLT extracellular vesiculomes but also on the characterization of a complex spectrum of PSLPs, that is, the DPLTs, PLT ghosts, fragments, and other different PLT membranous particles present

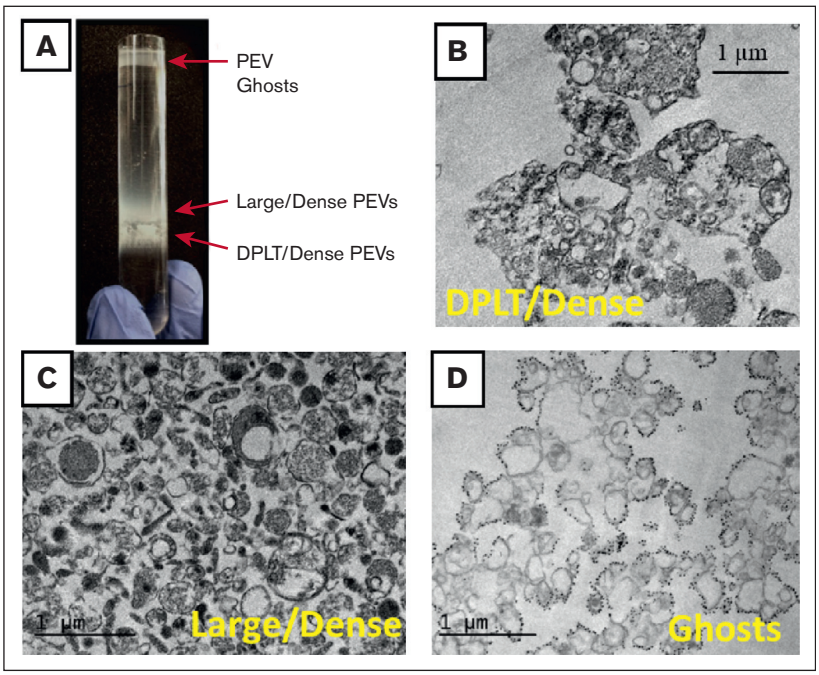

Figure 4. Ultrastructural analysis of PSLPs isolated by density gradient. (A) PSLPs from apheresis PLTs stored for 7 days float in a sucrose density gradient in 3 distinct populations. TEM images of PSLP population collected at (B) $d = 1.14$ to 1.17 g/mL band composed of DPLT and dense PEVs, (C) $d = 1.09$ to 1.13 g/mL band composed of large/dense PEVs, and (D) $d = 1.02$ to 1.06 g/mL composed of ghosts PEVs: membranous vesicles that float to the top of the density gradient. Apheresis PLTs were centrifuged at 1000 *g* for 30 minutes; the supernatant containing the PSLPs was fixed with 1% paraformaldehyde, pelleted (30 000 *g* for 20 minutes), and subjected to a sucrose density gradient for 14 hours.

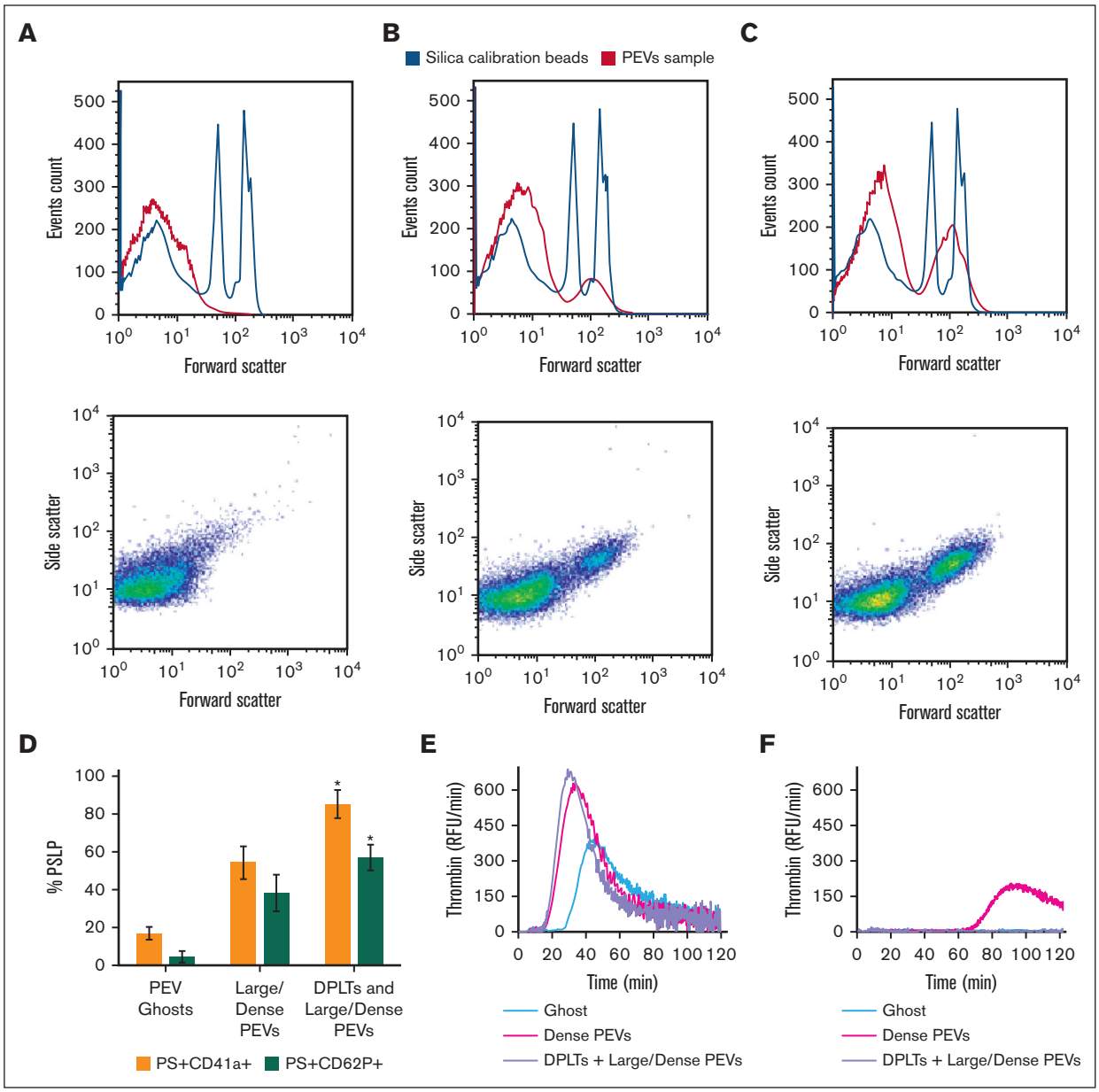

Figure 5. FC analysis of PSLP populations isolated by density gradient. Distribution and scatter plots of (A) PEV ghosts, (B) large/dense PEVs, and (C) DPLTs and large/dense PEVs. FC analysis of percentage of PS+CD62P+ PSLPs and PS+CD41a+ PSLPs present in the PSLP populations isolated by density gradient (D). N = 3, *t* test; $P < .05$ considered significant. TG assay demonstrates the procoagulant activities of PSLP populations isolated by sucrose density gradient. TG curves for PSLPs in the absence (E) and presence of 10 µmol/L of lactadherin (F), representative of 3 individual experiments and 3 individual donors. The same volume (50 µL) of each PSLP fraction was used in the experiment. RFU, relative fluorescence units.

in the apheresis PLT products stored at RT for transfusion. This article excludes the protein particles that may form during apheresis PLT storage.

TEM is considered the gold standard technique to evaluate the morphological features of cell death,[42,43] including autophagy.[44] Here, TEM revealed that the number of apoptotic and necrotic PLTs in apheresis PLT products increases with storage time and that mitophagy is operational in stored PLTs. We propose that these cell death processes contribute to the PSLP formation during storage of apheresis PLTs.

Apheresis procedures and storage of concentrated PLTs in bags expose PLTs to several stress factors, including contact with artificial surfaces, chemical changes caused by anticoagulants and additive solutions, metabolic stress, and shear stress, which collectively induce PLT activation and signaling leading to PLT apoptosis.[45] In agreement with that, our data show that stored PLTs undergo membrane remodeling, as evidenced by the increase in membrane fluidity and other structural changes (observed by electron microscopy) that are hallmarks of PLT activation: degranulation, pseudopodia formation, and PEV

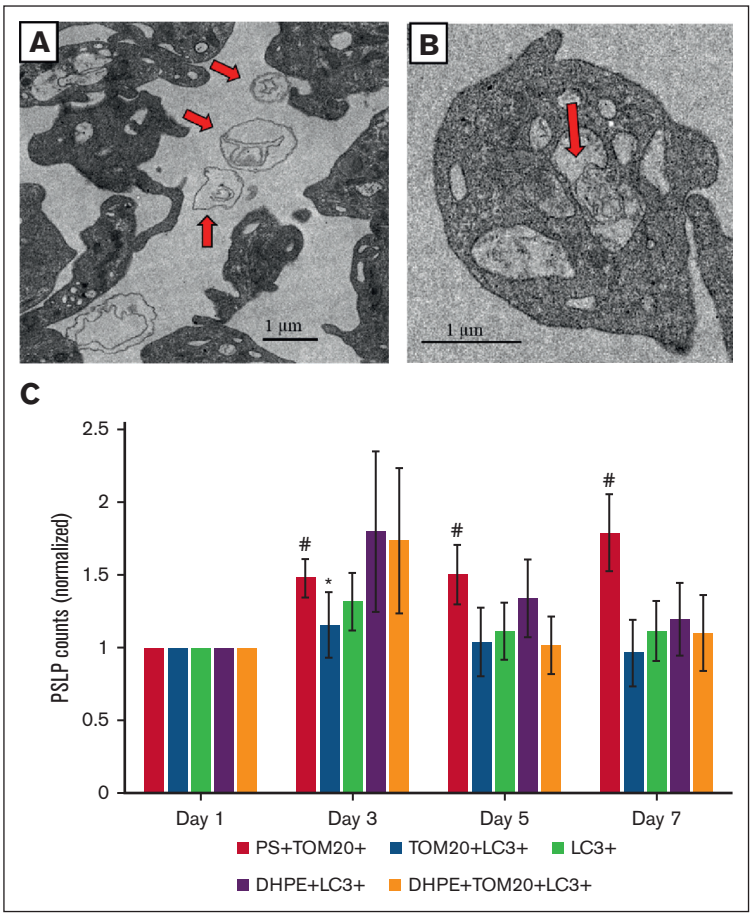

Figure 6. Apheresis PLTs release mitochondria (MITO) during storage at RT. TEM image of (A) extracellular MITO in apheresis PLT supernatant on day 7 of storage and (B) a mitochondrion in an autophagic vacuole. Red arrows indicate mitochondria. FC analysis of (C) $PS^+TOM20^+TOM20^+LC3^+$, $DHPE^+LC3^+$, and $DHPE^+TOM20^+LC3^+$ PSLPs. There is an increase in PS^+TOM20^+ PSLPs with storage time. The counts of mitophagy-related PSLPs do not significantly change during storage. FC data are expressed as the fold change in the count of small and large PEVs normalized to that of from day 1 PLT bag (mean ± SE) (#$P < .01$; *$P < .05$; N = 12).

release.[41,46] However, PSLPs are not composed only of PEVs from PLT activation during storage.

The density gradient allowed for the isolation of 3 major populations of PSLPs that are composed of DPLTs, PEVs, and PEV ghosts. TEM revealed that the DPLTs are PLTs with intact membranes that partially release the granule contents. DPLTs also include necrotic PLTs,[15] that is, PLTs that lost some of the internal organelles due to membrane fragmentation as observed by TEM. The tendency of apheresis PLT membranes to undergo fragmentation was also indicated by the membrane fluidity assay; the observed increase in membrane fluidity suggests that PLT membranes are less organized and viscous and thus more susceptible to lysis.[47] The large/dense PEV populations encompass the PEVs from PLT activation[41] and organelles from the fragmented necrotic PLTs. PSLPs include the PEV ghosts isolated at the very low-density band, which are electron translucent. That indicates that the PEV ghosts are remnant PEVs after the release of their internal contents. TEM and SEM allowed visualization of PSLPs with fragmented membranes, especially after day 3 of storage. Aside from the shear stress, proteolysis is known to induce membrane destabilization and fragmentation.[48] Indeed, extensive proteolysis in stored PLTs has been demonstrated,[49] and it has been associated with apoptosis.[50,51] In addition, FC analysis shows that the percentage of CD41a+ and CD62P+ in PEV ghosts is reduced as compared with in denser PEV and DPLT populations. Shedding of CD41a, CD62P epitopes due to proteolysis during storage has been reported previously.[26,52] Noteworthy, PLT ghosts[41] were also occasionally observed, indicating that the number of completely exhausted apheresis PLTs is relatively small during the storage up to 7 days.

FC analysis of PSLPs revealed 2 major PSLP populations distinguished by size distribution. Particle numbers of small and large PSLP populations steadily increase with storage time, as quantified by PS+ PSLPs and PS+CD41a+ PSLPs. The small PSLP population is composed of PEVs and PEV ghosts, as the sizes are <700 nm; the large PSLP populations are apoptotic and necrotic PLTs, PLT ghosts, and potentially other PSLP aggregates. Although we used well-established, relatively gentle methods for separation of platelets and PSLPs to minimize preanalytical platelet activation and alteration of PSLPs, we cannot fully exclude the impact of centrifugation and sucrose density gradient separation on PLT activation status and PSLP profile. Therefore, alternative PSLP separation methods should be explored in future studies.[53,54]

Interestingly, the number of small PS+CD62P+ PSLPs increases from days 1 to 3 only. Upon activation, platelet P-selectin (CD62P) is rapidly mobilized from α-granules to the platelet surface, a process that requires adenosine triphosphate. However, stored platelets experience a dramatic decrease in mitochondrial

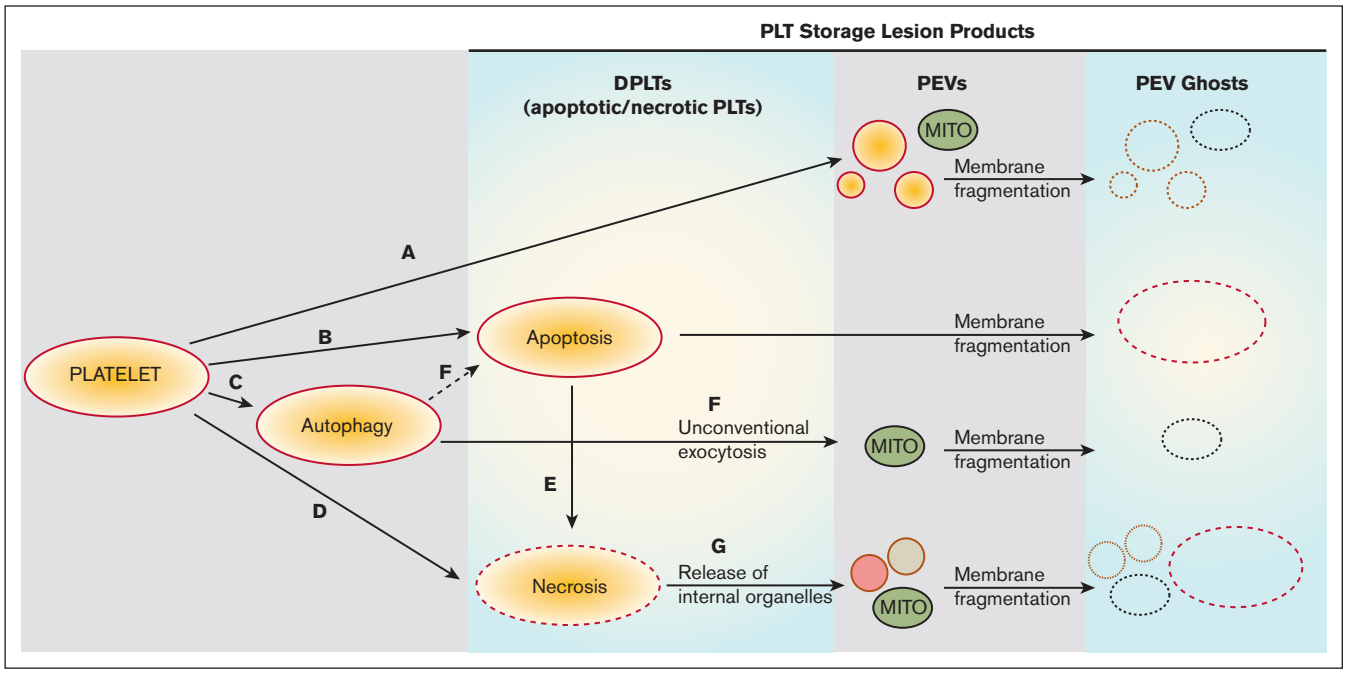

Figure 7. Proposed evolution of PSLP generation during storage of apheresis PLTs at RT. PSL leads to PLT activation with consequent release of PEVs (A) and induction of apoptosis (B), autophagy (C), and necrosis (D). Secondary necrosis may occur (E); autophagy may lead to apoptosis (F). These processes lead to accumulation of necrotic and apoptotic PLTs (DPLTs) during storage of apheresis PLTs at RT. The release of free mitochondria occurs through (A) PLT activation, (F) from unconventional exocytosis of autophagic vacuoles and (G) from necrotic PLTs, which releases organelles due to membrane fragmentation. Apoptotic and necrotic PLTs as well as PEVs, which include free mitochondria (MITO) and other organelles, became PEV ghosts because of storage-induced membranes fragmentation and leakage of internal contents.

respiration, and adenosine triphosphate depletion initiates within the first 2 days of storage.[55] Thus, a lack of further increase in PS+CD62P+ PSLP counts after day 3 of storage likely indicates a decline in PLT activation potency.

It has been shown that activated[56] and stored PLTs[57] release free MITO, and we showed previously that PLTs activated by the thrombin receptor activating peptide release MITO by different mechanisms.[41] In this study, we observed that stored apheresis PLTs contain extracellular MITO with damaged cristae and swollen structures, as presented in apoptotic and necrotic cells.[16-18,58] That is in agreement with a study by Perales Villarroel et al demonstrating that PLT storage time is associated with mitochondrial dysfunction and impaired PLT function.[55] Our FC analysis of PSLPs shows an increase in PS^+TOM20^+ PSLPs, which refers to the free MITO released upon PLT activation and MITO released from necrotic PLTs. Because of the membrane fragmentation, the large PS^+TOM20^+ PSLPs stemming from necrotic PLTs, and their count steadily increases with the storage time.

We identified PEVs that are products of mitophagy ($TOM20^+LC3^+$ PEVs), possibly released through unconventional exocytosis of autophagic vacuoles.[41,59] Interestingly, an increase in $DHPE^{+-}TOM20^+LC3^+$ PSLP counts during early storage was observed in 50% of donors, who all had lower PSLP counts on day 1 of storage. That indicates that longer storage does not increase mitophagy and that the release of the most of mitophagy-related PEVs exhausts by day 1 of storage.

In conclusion, we propose that the PSLPs are generated by multifactorial stress of PLTs, including contact, metabolic, and shear stress-induced PLT activation[60] and consequent cross-connections[61] with apoptosis,[43,45,50,62] necrosis,[7,15,63] and autophagy.[21,23,24] It has been demonstrated that different types of agitation affect platelet storage lesions, including activation status and PEV release.[64-66] Flatbed agitation, used in our study, is commonly used for platelet storage today but represents significantly higher shear stress for platelets, compared with slow (3 RPM) circulatory agitation.[67] Further studies are needed to evaluate how different types of agitation affect the activation status of PLTs and the quantitative profile of PSLPs, particularly PEVs. More gentle circulatory agitation should be investigated in this respect.

Our results suggest that different types of PSLPs are formed from functionally stimulated platelets and dying platelets. The activation-related PSLPs, including PEVs, are released particularly during the early stages of storage (days 1-3) and the release of apoptosis- and necrosis-related PSLPs prevails after that. A major challenge for the future will be the development of techniques to accurately analyze the contribution of distinct cell death pathways to PSLPs. The impact of these different PSLP populations on vascular endothelial cells and other relevant blood cells warrants future investigation. Although our study characterizes the morphology of the PSLPs in detail, further studies are needed on platelet storage-induced morphological and phenotype changes with the rate of their clearance from circulation and how different populations of PSLPs contribute to the hemostatic efficacy of transfused PLT units.

There are no ultimate data available on how PLT changes due to storage lesions affect their clinical transfusion performance. It has

been shown, however, that administration of fresh PLTs, less than 2 to 3 days stored, was associated with a significant increase in corrected count increment compared with older PLTs in 7 out of the 8 studies, although (except 1 retrospective study) there was no impact on bleeding events.[68] For full understanding of the biological effects of different PSLPs in circulation, in vivo studies in animal models would be useful. Activation, necrotic, and apoptotic PLT changes observed in our and other studies during storage well explain the decrease in in vivo bioavailability (recovery/survival) of longer-stored PLTs after transfusion. In contrast, observed procoagulant phenotype of longer-stored PLTs and the formation of procoagulant PSLPs support the hemostatic clinical efficacy of longer-stored platelets, which is in accord with the lack of an increase in bleeding complications with the time of PLT storage. The impact of these different PSLP populations on vascular endothelial cells and other relevant blood cells warrants future investigation to translate our findings into functional and clinical applications and to fully understand the functional significance of transfused PSLPs in vivo and their potential biomarker role in the evaluation of the quality of PLT transfusion products.

Acknowledgments

This project was supported in part by appointments to the Research Participation Program at the Center for Biologics Evaluation and Research administered by the Oak Ridge Institute for Science and Education through an interagency agreement between the US Department of Energy and the US Food and Drug Administration.

The findings and conclusions in this article have not been formally disseminated by the US Food and Drug Administration and should not be construed to represent any agency determination or policy.

Authorship

Contribution: M.P. wrote the manuscript and performed FC and fluorescent microscopy; S.H.D.P. wrote the manuscript and performed TEM, SEM, and density gradient; O.K.E. performed samples preparation and nanoparticle tracking analysis; I.D.T. performed membrane fluidity assay and edited the manuscript and figures; T.Z.T. performed TG assay; and J.S. supervised the project and revised the manuscript.

Conflict-of-interest disclosure: The authors declare no competing financial interests.

ORCID profile: S.H.D.P., 0000-0001-9197-8263.

Correspondence: Jan Simak, Center for Biologics Evaluation and Research, US Food and Drug Administration, 10903 New Hampshire Ave, WO Bldg 52/72, Room 4210, Silver Spring, MD 20993-0002; email: jan.simak@fda.hhs.gov.

References

1. Roback J, Rae Combs M, Grossman B, Hillyer C, eds. *Technical Manual of the American Assoc of Blood Banks*. 16th ed. AABB; 2008.
2. Murphy S, Gardner FH. Platelet storage at 22 degrees C; metabolic, morphologic, and functional studies. *J Clin Invest*. 1971;50(2):370-377.
3. Holme S, Moroff G, Murphy S. A multi-laboratory evaluation of in vitro platelet assays: the tests for extent of shape change and response to hypotonic shock. Biomedical Excellence for Safer Transfusion Working Party of the International Society of Blood Transfusion. *Transfusion*. 1998;38(1):31-40.
4. Holme S, Vaidja K, Murphy S. Platelet storage at 22 degrees C: effect of type of agitation on morphology, viability, and function in vitro. *Blood*. 1978;52(2):425-435.
5. Seghatchian J, Krailadsiri P. The platelet storage lesion. *Transfus Med Rev*. 1997;11(2):130-144.
6. Black A, orsó E, Kelsch R, et al. Analysis of platelet-derived extracellular vesicles in plateletpheresis concentrates: a multicenter study. *Transfusion*. 2017;57(6):1459-1469.
7. Jackson SP, Schoenwaelder SM. Procoagulant platelets: are they necrotic? *Blood*. 2010;116(12):2011-2018.
8. McArthur K, Chappaz S, Kile BT. Apoptosis in megakaryocytes and platelets: the life and death of a lineage. *Blood*. 2018;131(6):605-610.
9. Mason KD, Carpinelli MR, Fletcher JI, et al. Programmed anuclear cell death delimits platelet life span. *Cell*. 2007;128(6):1173-1186.
10. Nayak MK, Kulkarni PP, Dash D. Regulatory role of proteasome in determination of platelet life span. *J Biol Chem*. 2013;288(10):6826-6834.
11. Quach ME, Chen W, Li R. Mechanisms of platelet clearance and translation to improve platelet storage. *Blood*. 2018;131(14):1512-1521.
12. Schoenwaelder SM, Yuan Y, Josefsson EC, et al. Two distinct pathways regulate platelet phosphatidylserine exposure and procoagulant function. *Blood*. 2009;114(3):663-666.
13. Leytin V, Freedman J. Platelet apoptosis in stored platelet concentrates and other models. *Transfus Apher Sci*. 2003;28(3):285-295.
14. Bertino AM, Qi XQ, Li J, Xia Y, Kuter DJ. Apoptotic markers are increased in platelets stored at 37 degrees C. *Transfusion*. 2003;43(7):857-866.
15. Hua VM, Abeynaike L, Glaros E, et al. Necrotic platelets provide a procoagulant surface during thrombosis. *Blood*. 2015;126(26):2852-2862.
16. Remenyi G, Szasz R, Friese P, Dale GL. Role of mitochondrial permeability transition pore in coated-platelet formation. *Arterioscler Thromb Vasc Biol*. 2005;25(2):467-471.
17. Jobe SM, Wilson KM, Leo L, et al. Critical role for the mitochondrial permeability transition pore and cyclophilin D in platelet activation and thrombosis. *Blood*. 2008;111(3):1257-1265.
18. Zong WX, Thompson CB. Necrotic death as a cell fate. *Genes Dev*. 2006;20(1):1-15.

19. Rosenbalm KE, Lee-Sundlov MM, Ashline DJ, et al. Characterization of the human platelet N- and O-glycome upon storage using tandem mass spectrometry. *Blood Adv*. 2023;7(16):4278-4290.
20. Kroemer G, Levine B. Autophagic cell death: the story of a misnomer. *Nat Rev Mol Cell Biol*. 2008;9(12):1004-1010.
21. Ouseph MM, Huang Y, Banerjee M, et al. Autophagy is induced upon platelet activation and is essential for hemostasis and thrombosis. *Blood*. 2015; 126(10):1224-1233.
22. Zhang W, Ren H, Xu C, et al. Hypoxic mitophagy regulates mitochondrial quality and platelet activation and determines severity of I/R heart injury. *Elife*. 2016;5:e21407.
23. Lee SH, Du J, Stitham J, et al. Inducing mitophagy in diabetic platelets protects against severe oxidative stress. *EMBO Mol Med*. 2016;8(7):779-795.
24. Feng W, Chang C, Luo D, et al. Dissection of autophagy in human platelets. *Autophagy*. 2014;10(4):642-651.
25. He AD, Xie W, Song W, et al. Platelet releasates promote the proliferation of hepatocellular carcinoma cells by suppressing the expression of KLF6. *Sci Rep*. 2017;7(1):3989.
26. Cognasse F, Boussoulade F, Chavarin P, et al. Release of potential immunomodulatory factors during platelet storage. *Transfusion*. 2006;46(7): 1184-1189.
27. Sut C, Hamzeh-Cognasse H, Arthaud CA, et al. Platelet concentrate supernatants alter endothelial cell mRNA and protein expression patterns as a function of storage length. *Transfusion*. 2018;58(11):2635-2644.
28. Foged C, Brodin B, Frokjaer S, Sundblad A. Particle size and surface charge affect particle uptake by human dendritic cells in an in vitro model. *Int J Pharm*. 2005;298(2):315-322.
29. He C, Hu Y, Yin L, Tang C, Yin C. Effects of particle size and surface charge on cellular uptake and biodistribution of polymeric nanoparticles. *Biomaterials*. 2010;31(13):3657-3666.
30. Yue H, Wei W, Yue Z, et al. Particle size affects the cellular response in macrophages. *Eur J Pharm Sci*. 2010;41(5):650-657.
31. Zhang Y, Yang M, Park JH, et al. A surface-charge study on cellular-uptake behavior of F3-peptide-conjugated iron oxide nanoparticles. *Small*. 2009; 5(17):1990-1996.
32. Albanese A, Tang PS, Chan WC. The effect of nanoparticle size, shape, and surface chemistry on biological systems. *Annu Rev Biomed Eng*. 2012;14: 1-16.
33. Andar AU, Hood RR, Vreeland WN, Devoe DL, Swaan PW. Microfluidic preparation of liposomes to determine particle size influence on cellular uptake mechanisms. *Pharm Res*. 2014;31(2):401-413.
34. Laffont B, Corduan A, Plé H, et al. Activated platelets can deliver mRNA regulatory Ago2*microRNA complexes to endothelial cells via microparticles. *Blood*. 2013;122(2):253-261.
35. Rumbaut RE, Thiagarajan P. Platelet-Vessel Wall Interactions in Hemostasis and Thrombosis. *Morgan & Claypool Life Sciences*. 2010.
36. Schneider CA, Rasband WS, Eliceiri KW. NIH image to ImageJ: 25 years of image analysis. *Nat Methods*. 2012;9(7):671-675.
37. Tegegn TZ, De Paoli SH, Orecna M, et al. Characterization of procoagulant extracellular vesicles and platelet membrane disintegration in DMSO-cryopreserved platelets. *J Extracell Vesicles*. 2016;5:30422.
38. Standards for blood banks and transfusion services. *QRB Qual Rev Bull*. 1977;3(12):17-22.
39. Acker J RA, Marks D. Whole blood and apheresis collection of blood components intended for transfusion. In: Cohn CS DM, Johnson ST, Katz LM, Schwartz J, eds. *Technical Manual*. 21st ed. 2023:137-168. AABB.
40. do Canto A, Robalo JR, Santos PD, Carvalho AJP, Ramalho JPP, Loura LMS. Diphenylhexatriene membrane probes DPH and TMA-DPH: a comparative molecular dynamics simulation study. *Biochim Biophys Acta*. 2016;1858(11):2647-2661.
41. De Paoli SH, Tegegn TZ, Elhelu OK, et al. Dissecting the biochemical architecture and morphological release pathways of the human platelet extracellular vesiculome. *Cell Mol Life Sci*. 2018;75(20):3781-3801.
42. Tinari A, Giammarioli AM, Manganelli V, Ciarlo L, Malorni W. Analyzing morphological and ultrastructural features in cell death. *Methods Enzymol*. 2008; 442:1-26.
43. Zhang Y, Chen X, Gueydan C, Han J. Plasma membrane changes during programmed cell deaths. *Cell Res*. 2018;28(1):9-21.
44. Klionsky DJ, Abdelmohsen K, Abe A, et al. Guidelines for the use and interpretation of assays for monitoring autophagy (3rd edition). *Autophagy*. 2016; 12(1):1-222.
45. Leytin V, Allen DJ, Mykhaylov S, et al. Pathologic high shear stress induces apoptosis events in human platelets. *Biochem Biophys Res Commun*. 2004; 320(2):303-310.
46. Rijkers M, van den Eshof BL, van der Meer PF, et al. Monitoring storage induced changes in the platelet proteome employing label free quantitative mass spectrometry. *Sci Rep*. 2017;7(1):11045.
47. Shattil SJ, Cines DB, Schreiber AD. Increased fluidity of human platelet membranes during complement-mediated immune platelet injury. *J Clin Invest*. 1978;61(3):582-589.
48. Besingi RN, Clark PL. Extracellular protease digestion to evaluate membrane protein cell surface localization. *Nat Protoc*. 2015;10(12):2074-2080.
49. Prudova A, Serrano K, Eckhard U, Fortelny N, Devine DV, Overall CM. TAILS N-terminomics of human platelets reveals pervasive metalloproteinase-dependent proteolytic processing in storage. *Blood*. 2014;124(26):e49-60.

50. Zhao L, Liu J, He C, et al. Protein kinase A determines platelet life span and survival by regulating apoptosis. *J Clin Invest*. 2017;127(12):4338-4351.
51. Perrotta PL, Perrotta CL, Snyder EL. Apoptotic activity in stored human platelets. *Transfusion*. 2003;43(4):526-535.
52. Andrews RK, Gardiner EE. Basic mechanisms of platelet receptor shedding. *Platelets*. 2017;28(4):319-324.
53. Thery C, Amigorena S, Raposo G, Clayton A. Isolation and characterization of exosomes from cell culture supernatants and biological fluids. *Curr Protoc Cell Biol*. 2006;30(1); Chapter 3: unit 3 22.
54. Momen-Heravi F, Balaj L, Alian S, et al. Current methods for the isolation of extracellular vesicles. *Biol Chem*. 2013;394(10):1253-1262.
55. Perales Villarroel JP, Figueredo R, Guan Y, et al. Increased platelet storage time is associated with mitochondrial dysfunction and impaired platelet function. *J Surg Res*. 2013;184(1):422-429.
56. Boudreau LH, Duchez AC, Cloutier N, et al. Platelets release mitochondria serving as substrate for bactericidal group IIA-secreted phospholipase A2 to promote inflammation. *Blood*. 2014;124(14):2173-2183.
57. Marcoux G, Duchez AC, Rousseau M, et al. Microparticle and mitochondrial release during extended storage of different types of platelet concentrates. *Platelets*. 2017;28(3):272-280.
58. Sun MG, Williams J, Munoz-Pinedo C, et al. Correlated three-dimensional light and electron microscopy reveals transformation of mitochondria during apoptosis. *Nat Cell Biol*. 2007;9(9):1057-1065.
59. Pfeffer SR. Unconventional secretion by autophagosome exocytosis. *J Cell Biol*. 2010;188(4):451-452.
60. Pang A, Cui Y, Chen Y, et al. Shear-induced integrin signaling in platelet phosphatidylserine exposure, microvesicle release, and coagulation. *Blood*. 2018;132(5):533-543.
61. Eisenberg-Lerner A, Bialik S, Simon HU, Kimchi A. Life and death partners: apoptosis, autophagy and the cross-talk between them. *Cell Death Differ*. 2009;16(7):966-975.
62. Leytin V. Apoptosis in the anucleate platelet. *Blood Rev*. 2012;26(2):51-63.
63. Zhang Y, Zhang J, Yan R, et al. Receptor-interacting protein kinase 3 promotes platelet activation and thrombosis. *Proc Natl Acad Sci U S A*. 2017;114(11):2964-2969.
64. Snyder EL, Koerner TA Jr, Kakaiya R, Moore P, Kiraly T. Effect of mode of agitation on storage of platelet concentrates in PL-732 containers for 5 days. *Vox Sang*. 1983;44(5):300-304.
65. George JN, Pickett EB, Heinz R. Platelet membrane glycoprotein changes during the preparation and storage of platelet concentrates. *Transfusion*. 1988;28(2):123-126.
66. Hosseini E, Solouki A, Haghshenas M, Ghasemzadeh M, Schoenwaelder SM. Agitation-dependent biomechanical forces modulate GPVI receptor expression and platelet adhesion capacity during storage. *Thromb J*. 2022;20(1):3.
67. Torres R, Tormey CA, Stack G. Fluid motion and shear forces in platelet storage bags with different modes of agitation. *Vox Sang*. 2016;111(2):209-212.
68. Aubron C, Flint AWJ, Ozier Y, McQuilten Z. Platelet storage duration and its clinical and transfusion outcomes: a systematic review. *Crit Care*. 2018;22(1):185.